Proceedings of the ASME 2018 37th International
Conference on Ocean, Offshore and Arctic Engineering
OMAE2018
June 17-22, 2018, Madrid, Spain

OMAE2018-78388

Kriging-Based Surrogate Model Combined with Weighted Expected Improvement for Ship Hull Form Optimization

Xinwang Liu
Collaborative Innovation Center for Advanced Ship and Deep-Sea Exploration, State Key Laboratory of Ocean Engineering, School of Naval Architecture, Ocean and Civil Engineering, Shanghai Jiao Tong University, Shanghai 200240, China

Decheng Wan*
Collaborative Innovation Center for Advanced Ship and Deep-Sea Exploration, State Key Laboratory of Ocean Engineering, School of Naval Architecture, Ocean and Civil Engineering, Shanghai Jiao Tong University, Shanghai 200240, China
*Corresponding author: dcwan@sjtu.edu.cn

Gang Chen
Collaborative Innovation Center for Advanced Ship and Deep-Sea Exploration, State Key Laboratory of Ocean Engineering, School of Naval Architecture, Ocean and Civil Engineering, Shanghai Jiao Tong University, Shanghai 200240, China

ABSTRACT

The paper explores Kriging-based surrogate model combined with Weighted Expected Improvement approach and for the ship hull form optimization. The training dataset of the Kriging-based surrogate model is obtained by sampling the design space (Design of Experiments, DOE) and performing expensive high-fidelity computations on the selected points. Expected Improvement (EI) is used as a criterion to select one additional sample point in each iteration. The Weighted Expected Improvement (WEI) is derived from EI by adding a tunable parameter which can adjust the weights on exploration and exploitation in the Efficient Global Optimization(EGO).

The proposed method selects more than one new sample point by changing the weight parameter for each optimization iteration, thus it can be performed by parallel computation or multi-computer runs which improves the computational efficiency distinctly. This makes it possible not only to improve the accuracy of the surrogate model, but also to explore the global optimum much more quickly. The present method is applied to mathematical test function and a ship hull form optimization design in order to find the optimal hull form with best resistance performance in calm water in different speeds.

The result shows that the criterion of WEI can be applied in EGO for optimization design and can be easily extended to other hull form optimization design problems based on computational fluid dynamics.

KEYWORDS

Kriging model; Weighted Expected Improvement; Efficient Global Optimization; Hull form optimization

INTRODUCTION

In the process of ship design, hull form design is of vital importance. The design level of ship hull form has a great influence on its hydrodynamic performances and economic efficiency of the ship. In recent years, with the vigorous development of computer technology and the continuous improvement of the calculation theory, the Simulation-Based-Design (SBD) technology is becoming possible. It is a new design method which integrates hull form transformation method, optimization technology and numerical calculation module. The technique uses geometric reconstruction method to transform and express hull form, and then predicts the hydrodynamic performance of each hull form scheme with computational fluid dynamic methods. Finally, the optimal hull satisfying the constraint condition is obtained by the optimization algorithm. In order to greatly save the high computational cost, one alternative method is to construct a relatively simple surrogate model instead of the complicated numerical analysis of a large number of sample points in order to find the relationship, which is often with strong nonlinearity, between the design variables (input) and the objective functions (output). The surrogate model expresses the relationship between the design variables and the objective functions using a stochastic Gaussian process. The model requires very little time to evaluate the objective function. The most widely used surrogate model are the polynomial-based model, the response surface model, the Kriging model.

The Kriging model can predict the value of the unknown point using stochastic processes (1), and it has gained popularity for the ship hull form optimization design. However, it is possible to miss the global optimum in the searching space if we only rely on the prediction value of the Kriging model because the model includes uncertainty at each point unless the sample points that have been used to construct the Kriging model. For robust exploration of the global optimum point, both the prediction value and its uncertainty should be considered at the same time. This concept is expressed in the criterion expected improvement (EI). EI includes the probability of a point being optimum in the design space. By the selection of the best EI point as the additional sample point, improvement of the model and robust exploration of the global optimum can be achieved at the same time, which is called Efficient Global Optimization (EGO) (2).

The statistical framework of Kriging provides an estimator of the variance of the Kriging interpolator. Using this potential error, different metrics have been proposed to adaptively change the sample points in the design space such that the deterministic optimum of an unconstrained problem can be found efficiently. Expected Improvement (EI) has been shown to be sound statistical infill sampling criteria. By constructing an initial model using a suitable DoE (3) and then implementing EI, Jones et al. showed that the deterministic global optimum of an unconstrained problem can be found using relatively few expensive simulations and used the term Efficient Global Optimization to refer to this method (2). The EI algorithm distributes the weights equally between the two terms and can be seen as a fixed compromise between exploration and exploitation. In order to study the effect of different weights, the Weighted Expected Improvement(WEI) (2) was derived from EI by adding a tunable weighting parameter. In this article, EGO method that WEI is applied in will be applied to the ship hull form optimization design of KRISO Container Ship.

THEORY OF KRIGING MODEL AND WEI

As a kind of regression model, Kriging model (4) is able to exploit the spatial correlation of data in order to predict the shape of the objective function based only on limited information. Kriging exploits the spatial correlation of data in order to build interpolation; therefore, the correlation function is a critical element. This model combines a global model and a local component:

$$y(\mathbf{x}) = f(\mathbf{x}) + z(\mathbf{x}) \tag{1}$$

where $y(\mathbf{x})$ is the unknown real function, $f(\mathbf{x})$ is a known approximation function, and $z(\mathbf{x})$ is the realization of a stochastic process with mean zero, variance σ^2, and non-zero covariance. With $f(\mathbf{x})$ and $z(\mathbf{x})$, the Kriging model can be built to represent the relationship between the input variables and output variables.

The Kriging predictor is given by:

$$\hat{y} = \hat{\beta} + \mathbf{r}^T(\mathbf{x})\mathbf{R}^{-1}\left(\mathbf{y} - \mathbf{f}\hat{\beta}\right) \tag{2}$$

where $\hat{y}$ is an n_s-dimensional vector that contains the sample values of the response; $\mathbf{f}$ is a column vector of length n_s that is filled with ones when $\mathbf{f}$ is taken as a constant; $\mathbf{r}^T(\mathbf{x})$ is the correlation vector of length n_s between an untried $\mathbf{x}$ and the sampled data points $\left\{\mathbf{x}^{(1)}, \mathbf{x}^{(2)}, \cdots, \mathbf{x}^{(n_s)}\right\}$ and is expressed as:

$$\mathbf{r}^T(\mathbf{x}) = \left[R\left(\mathbf{x}, \mathbf{x}^{(1)}\right), R\left(\mathbf{x}, \mathbf{x}^{(2)}\right), \cdots, R\left(\mathbf{x}, \mathbf{x}^{(n_s)}\right)\right]^T \tag{3}$$

Additionally, the Gaussian correlation function is employed in this work:

$$R\left(x^i, x^j\right) = \exp\left[-\sum_{k=1}^{n_{dv}} \theta_k \left|x_k^i - x_k^j\right|^2\right] \tag{4}$$

In equation (2), $\hat{\beta}$ is estimated using equation (5):

$$\hat{\beta} = \left(\mathbf{f}^T\mathbf{R}^{-1}\mathbf{f}\right)^{-1}\mathbf{f}^T\mathbf{R}^{-1}\mathbf{y} \tag{5}$$

The estimate of the variance $\hat{\sigma}^2$, between the underlying global model $\hat{\beta}$ and $\mathbf{y}$ is estimated using equation (6):

$$\hat{\sigma}^2 = \left[\left(\mathbf{y} - \mathbf{f}\hat{\beta}\right)^T \mathbf{R}^{-1}\left(\mathbf{y} - \mathbf{f}\hat{\beta}\right)\right] \Big/ n_s \tag{6}$$

where $f(\mathbf{x})$ is assumed to be the constant $\hat{\beta}$. The maximum likelihood estimates for the θ_k in equation (4) used to fit a Kriging model are obtained by solving equation (7):

$$\max_{\theta_k > 0} \Phi\left(\theta_k\right) = -\left[n_s \ln\left(\hat{\sigma}^2\right) + \ln\left|\mathbf{R}\right|\right] \Big/ 2 \tag{7}$$

where both $\hat{\sigma}^2$ and $\mathbf{R}$ are functions of θ_k. While any value for the θ_k create an interpolative Kriging model, the "best" Kriging model is found by solving the *k*-dimensional unconstrained, nonlinear, optimization problem given by equation (7).

The accuracy of the prediction value largely depends on the distance from sample points. Intuitively speaking, the closer point $\mathbf{x}$ to the sample point, the more accurate is the prediction $\hat{y}$. This intuition is expressed as

$$s^2(\mathbf{x}) = \hat{\sigma}^2 \left[\mathbf{1} - \mathbf{r}^T \mathbf{R}^{-1} \mathbf{r} + \frac{(\mathbf{1} - \mathbf{1}\mathbf{R}^{-1}\mathbf{r})^2}{\mathbf{1}^T \mathbf{R}^{-1} \mathbf{1}} \right] \quad (8)$$

where $s^2(\mathbf{x})$ is the mean squared error of the predictor and it indicates the uncertainty at the estimation point. The root mean squared error (RSME) is expressed as $s = \sqrt{s^2(\mathbf{x})}$.

Since the Kriging model treats the target function as a Gaussian process, the value of an unknown point $\mathbf{x}$ can be regarded as a random value $y(\mathbf{x})$ of Gaussian distribution with mean $\hat{y}(\mathbf{x})$ and variance $s^2(\mathbf{x})$. Then the improvement of this point beyond the best observed value $f_{\min}$ is also a random value (2):

$$I(\mathbf{x}) = \max\left(y_{\min} - y(\mathbf{x}), 0\right) \quad (9)$$

The expected improvement criterion calculates the mathematic expectation of the improvement value, and can be derived in closed form

$$EI(\mathbf{x}) = \left(f_{\min} - \hat{y}(\mathbf{x})\right)\Phi\left[\left(f_{\min} - \hat{y}(\mathbf{x})\right)/s(\mathbf{x})\right] + s(\mathbf{x})\phi\left[\left(f_{\min} - \hat{y}(\mathbf{x})\right)/s(\mathbf{x})\right] \quad (10)$$

Where $f_{\min}$ is the minimum value among n_s sampled values. Φ and ϕ are the standard distribution and normal density, respectively.

It is easy for us to get the simple following expressions:

$$\frac{\partial EI}{\partial \hat{y}} < 0, \frac{\partial EI}{\partial s} < 0 \quad (11)$$

It turns out that EI is monotonic in $\hat{y}$ and in s. Thus, we see that the EI is larger the lower is $\hat{y}$ and the higher is s. By selecting the maximum EI point as additional sample point, robust exploration of the global optimum and improvement of the model can be achieved simultaneously. The beauty of the expected improvement function can be seen from Eq. (10) that it gives an elegant balance between local search and global search. The first term of Eq. (10), including Gaussian density, favors "exploitation"—searching the most promising regions (high confidence); while the second term, containing the Gaussian distribution, prefers "exploration"—searching the regions that have high uncertainty. The EGO algorithm chooses the point with the highest EI value to update the Kriging model and the EI function. After that the next candidate point can be selected based on the updated EI function.

The traditional EGO algorithm above has two main problems. Firstly, the traditional EGO algorithm can't get the second updating point without evaluating the first updating point because the EI function needs be updated by the first updating point. As a result, the traditional EGO algorithm can only evaluate the designs sequentially, not in a parallel way, which is a real waste of time, especially in the applications of high time-costing CFD-based hull form optimizations. Secondly, it has been found (5) that in some practical cases exploration performs dramatically better in terms of finding the global optimum, whereas exploitation often causes the Kriging model to stop around a local minimum. The termination criteria used by the Kriging model are often based on finding repeatedly the same sampling point within prescribed tolerance, thus balancing exploration and exploitation is vital. The EI algorithm distributes the weights equally between the two terms and can be seen as a fixed compromise between exploration and exploitation. In order to tackle the problem, the Weighted Expected Improvement (WEI) (2) was derived from EI by adding a tunable weighting parameter. Through a set of experiments, it was shown that by changing the value of the tunable parameter the efficiency of finding the global minimum can be affected.

$$WEI(\mathbf{x}, \omega) = \omega\left(f_{\min} - \hat{y}(\mathbf{x})\right)\Phi\left[\frac{\left(f_{\min} - \hat{y}(\mathbf{x})\right)}{s(\mathbf{x})}\right] + (1-\omega)s(\mathbf{x})\phi\left[\frac{\left(f_{\min} - \hat{y}(\mathbf{x})\right)}{s(\mathbf{x})}\right] \quad (12)$$

By changing the tunable weighting parameter $\omega \in [0,1]$, we can add new sample points in a parallel way, thus we can find a minimum closer to the real minimum of the objective function more quickly and ensure that the Kriging model has high fidelity.

MATHEMATICAL APPLICATION

A typical test problem is used for the experiment so that we do not need to worry the computational time. It is described below:

Six-hump camel-back function (Six-hump) with $n = 2$(6):

$$f(x, y) = 4x^2 - \frac{21}{10}x^4 + \frac{1}{3}x^6 + xy - 4y^2 + 4y^4 \quad (13)$$

where $(x, y) \in [-2, 2] \times [-2, 2]$.

Its graph is shown in Figure 1.

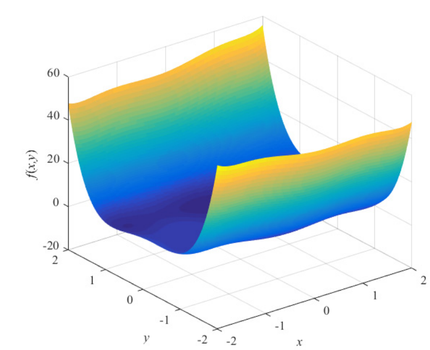

FIGURE.1 GRAPH OF SIXHUMP FUNCTION(2-DIM)

The OLHS technique is used to generate sample points in the design space to construct the Kriging model.

Method 1: If we use a small number of sample points to construct the Kriging model, then the graph will be like Figure 2.

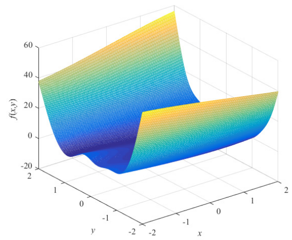

FIGURE.2 GRAPH OF SIXHUMP FUNCTION WITH 30 SAMPLE POINTS

Method 2:If we use a small number of sample points and take WEI into consideration to add new points in parallel($\omega \in \{0.1, 0.2, 0.3, 0.4, 0.5, 0.6, 0.7, 0.8, 0.9\}$) to construct the Kriging model, then the graph will be like Figure 2.

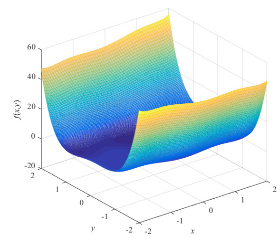

FIGURE. 3 GRAPH OF SIXHUMP FUNCTION WITH 30+18 SAMPLE POINTS

What's more, in addition to the evaluation of fidelity of the Kriging model, the cross validations for the models are performed and the results are shown in Figure 4 and 5. In the cross validation, each sample point is evaluated from the surrogate model that is constructed by the other sample points. It can be observed from Figure 5 that the calculated objective function values by Eq. (13) (f_{cal}) and estimated objective function values(f_{est}) given by the surrogate model show a better agreement than Figure 4.

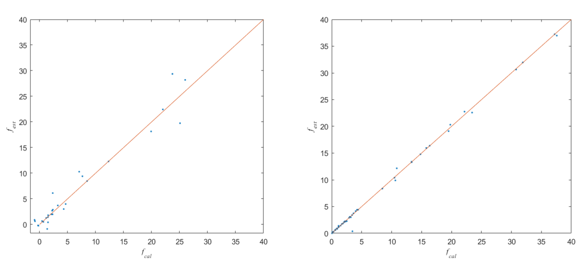

(A)METHOD 1 (B)METHOD 2

FIGURE.4 CROSS VALIDATIONS OF KRIGING MODEL BY METHOD 1 AND 2

If you don't use EGO method, you have to generate a large number of sample points to insure the accuracy of the Kriging model.

METHODS OF HULL FORM OPTIMIZATION DESIGN

Hull form optimization is a comprehensive technology with many links. It can be mainly divided into three parts: the deformation and expression of the hull form, the solution and evaluation of hydrodynamic performance, and the search and filter of the optimization algorithm.

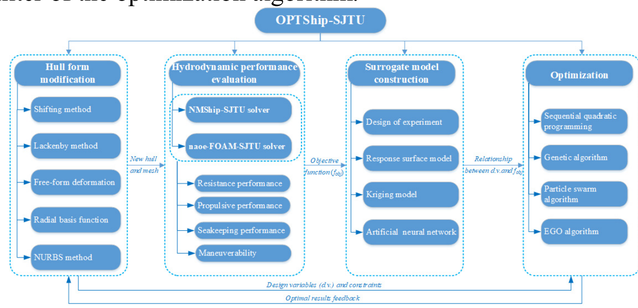

FIGURE.5 FRAMEWORK DIAGRAM OF OPTSHIP-SJTU

The OPTShip-SJTU solver is a self-developed tool based on C++ language for the ship hull form optimization, which has obtained national software copyright. It integrates with a hull surface modification module, a hydrodynamic performance evaluation module, a surrogate module and an optimization module, which can achieve the ship hull form optimization design automatically. The framework of OPTSHIP-SJTU can be seen in Figure 5.

1.Ship form transformation module—FFD method

Ship hull form transformation module is a bridge connecting ship performance evaluation module and optimization module. When the optimization module selects a new series of variables for the design, ship transformation module needs to make rapid response to the certain set of optimization design variables and send them to the ship hydrodynamic performance evaluation module, evaluation results will further affect the optimization module of design. The free surface deformation method FFD is a free mesh deformation method proposed by Sederberg and Parry (7)(8) in 1986. It has been widely used in various fields including hull geometry reconstruction and other transportation tools. The basic idea is as follows.

Firstly, a local coordinate system is constructed in a cube containing the object to be deformed. O '-STU constructs a local coordinate system, as shown in Fig. 1.

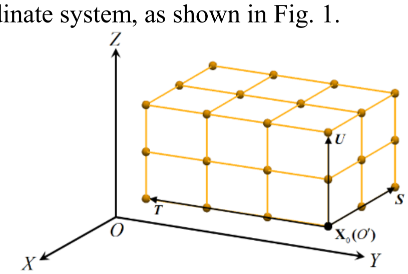

FIGURE.6 LOCAL COORDINATE SYSTEM OF FFD METHOD

Here, *O* is the origin of the local coordinate system, *S*, *T*, and *U* are axes vectors along three axes in the local coordinate system. It is obvious, such as the coordinates of *X* in Descartes *O-XYZ*, in a local coordinate system for (*s, t, U*), we have:

$$\mathbf{X} = \mathbf{X}_0 + s\boldsymbol{S} + t\boldsymbol{T} + u\boldsymbol{U} \tag{14}$$

where X_0 is the origin of the local coordinate system, and s, t, and u can be obtained as:

$$s = \frac{\boldsymbol{T}\times\boldsymbol{U}(\mathbf{X}-\mathbf{X_0})}{\boldsymbol{T}\times\boldsymbol{U}\cdot\boldsymbol{S}},\ t = \frac{\boldsymbol{S}\times\boldsymbol{U}(\mathbf{X}-\mathbf{X_0})}{\boldsymbol{S}\times\boldsymbol{U}\cdot\boldsymbol{T}},\ u = \frac{\boldsymbol{S}\times\boldsymbol{T}(\mathbf{X}-\mathbf{X_0})}{\boldsymbol{S}\times\boldsymbol{T}\cdot\boldsymbol{U}} \tag{15}$$

Obviously, the values of s, t, and u are between 0 and 1.

In cuboid structure, the control points $\boldsymbol{Q}_{i,j,k}$, can be easily got by the following expression and can be seen as yellow dots in Figure 6.

$$\boldsymbol{Q}_{i,j,k} = \boldsymbol{O}' + \frac{i}{l}\boldsymbol{S} + \frac{j}{m}\boldsymbol{T} + \frac{k}{n}\boldsymbol{U} \tag{16}$$

where $i = 0,1,\cdots,l;\ j = 0,1,\cdots,m;\ j = 0,1,\cdots,n.$

Therefore, any point **X** in the framework of Descartes coordinates can be controlled by the control points for:

$$\mathbf{X}(s,t,u) = \sum_{i=0}^{l}\sum_{j=0}^{m}\sum_{k=0}^{n} B_{i,l}(s)B_{j,m}(t)B_{k,n}(u)\boldsymbol{Q}_{i,j,k} \tag{17}$$

where B represents for the Bernstein polynomial basis function:

$$B_{i,n}(u) = \frac{n!}{i!(n-i)!}u^i(1-u)^{n-i} \tag{18}$$

It can be seen from Eq. (17) and (18) that the initial hull mesh is the linear function of all the control points. After setting up the relation between the geometry and the frame of the ship, we will take the position of some control nodes as the design optimization variables, and then achieve the goal of ship type transformation through the deformation of the control frame. Suppose that the local coordinates of the X in the original control framework are (s, t, u), and that the control points $\boldsymbol{Q}_{i,j,k}$ are changed to obtain new control nodes $\boldsymbol{Q'}_{i',j',k'}$, and then the point X will move to point $\mathbf{X}_{ffd}$:

$$\mathbf{X}_{ffd} = \sum_{i=0}^{l}\sum_{j=0}^{m}\sum_{k=0}^{n} B_{i,l}(s)B_{j,m}(t)B_{k,n}(u)\boldsymbol{Q}'_{i,j,k} \tag{19}$$

By changing the number, direction and size of the control points, different new meshes of the hull can be obtained.

2.Hydrodynamics performance evaluation module — NMSHIP-SJTU

Here, we need to evaluate the hydrodynamic performance of the wave-making resistance at Fr=0.26 and 0.35. We adopted the self-developed NM theory solver NMShip-SJTU based on a potential theory, Newmann-Mitchell theory to calculate the wave-making resistance. Neumann-Michell theory (NM theory) is proposed by Francis Noblesse et al based on the Neumann-Kelvin theory (NK theory) (9). NM theory eliminate the ship waterline integral item in the NK theory, and the whole calculation can be converted to the integral on the wet surface of the ship. The theory adopts the coordination linear flow model and there's no need to solve the distribution on the boundary of the source but calculate the wave resistance through the iteration of velocity potential. Besides, there are a lots of research about comparisons of experimental measurements of wave drag with numerical predictions obtained using the NM theory for the Wigley hull, the Series 60 and DTMB 5415 model. Zhang et al of our research group, self-developed the NMShip -SJTU solver based on NM theory and calculated the resistance of catamaran, including the resistance of Delft catamaran and Series 60 catamaran in different demihull spacings (10). The results showed that the calculation results are in good agreement with experimental measurements. Wu et al succeed to optimize hull form of Wigley with the best wave resistance performance evaluated by NM theory (11). Yang and Huang presented that the sum of the ITTC friction resistance and the NM theory wave resistance could be expected to yield realistic practical estimates, which could be useful for routine applications to design and ship hull form optimization of a broad range of displacement ships (12). The computation of the steady flow around a moving ship based on NM theory is efficient and robust due to the succinctness of this theory, and Kim et al pointed that the wave resistance predicted by NM theory is in fairly good agreement with experimental measurements (13). Using NM theory can quickly complete the resistance performance forecast on personal computers. Xinwang Liu and Decheng Wan regarded the quadramaran as the research object and successfully calculated the wave-making resistance by NMShip-SJTU solver(14).

3.Optimization module—MOGA-II

At the stage of computing optimization, we first select 20 sample points in the sample points in the design space by Optimal Latin Hypercube Sampling method (OLHS) design, and use the Kriging model instead of huge numerical calculation to make quick evaluation. Finally, the multi-objective genetic algorithm MOGA-II is selected as the optimization method, and after 300×200 individual evolutions, the ideal optimization scheme is obtained. MOGA-II, a multi-objective genetic algorithm, is implemented in many hull form optimization cases.

APPLICATION OF SHIP OPTIMIZATION DESIGN OF KCS

1.Objective functions

The optimal calculation in this paper takes the KCS as the parent ship, which has the ship main dimensions of L=7.3577m, B=1.03m, D=0.346m. There are 2 objective functions shown below. We hope the smaller of the two objective functions, the better, that is

$$f_{obj1} = \min\{C_w\}, Fr = 0.26$$

$$f_{obj2} = \min\{C_w\}, Fr = 0.35$$

2.Design variables

Optimization variables are used to control the free variation of the ship form in the design space. Ship transformation method in this paper is FFD method, involving two lattices (shown in Figure 7) at the bulbous bow and stern parts. Red points are movable while green points are fixed.

Four optimization design variables *X1, Y1, Z1, Y2* are summed up. The first 3 variables control the change of the bulbous bow surface in three directions: *x, y* and *z*. The last variable controls the change of the stern surface of the ship in the *y* direction. In order to ensure that the ship is within a reasonable range, the range of the variables is specified in Table 1.

TABLE 1: THE RANGE OF THE 5 VARIABLES

	Variables	Min	Max
Lattice-1	X1	-0.01	0.01
	Y1	-0.005	0.005
	Z1	-0.0015	0.0015
Lattice-2	Y2	-0.007	0.007

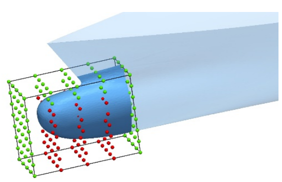

(A)BOW-X DIRECTION

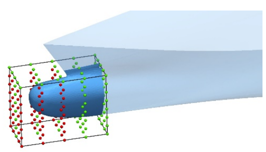

(B) BOW-Y DIRECTION

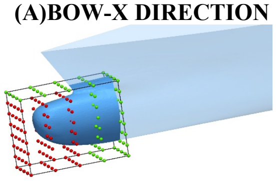

(C) BOW-Z DIRECTION

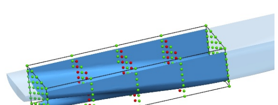

(D) STERN-Y DIRECTION

FIGURE.7 SCHEMATIC DIAGRAM OF FFD METHOD APPLICATION (LATTICE AND LAYOUT OF CONTROL POINTS)

3.Optimization results and analysis

Method 1: We firstly use the optimization of OLHS method to generate 60 sample points, they are uniformly distributed in the design space; then we set Kriging approximation model to do the optimization calculation. We select the multi-objective genetic algorithm NSGA- II as the optimization method, and calculate the 300×200 individuals to get the optimization results.

Each of the solutions in the resulting Pareto solution is a potential "optimal solution", and the difference between them is the trade-off between the two objective functions. The optimization results are shown in Figure 8. For ease of analysis, we choose 3 schemes from the Pareto solution set, and mark them as Case-1, Case-2 and Case-3 in the diagram. The optimization results corresponding to the initial hull are shown in Table 2.

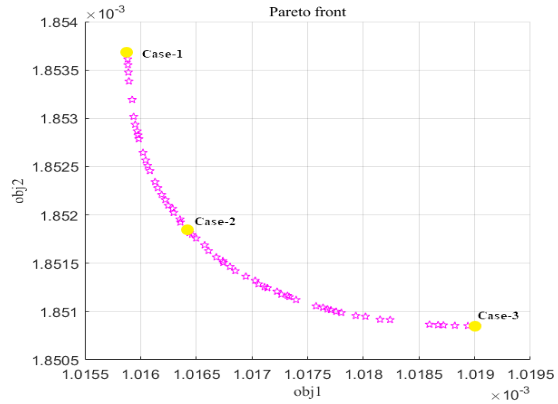

FIGURE.8 PARETO FRONT OF METHOD 1

TABLE.2 OPTIMIZATION RESULTS CORRESPONDING TO THE INITIAL HULL

	C_w (Fr=0.26)	C_w (Fr=0.35)
Initial	0.001211	0.002076
Case-1	0.001049	0.001888
Decrease percent	-13.39%	-9.02%
Case-2	0.001065	0.001899
Decrease percent	-12.04%	-8.52%
Case-3	0.001087	0.001913
Decrease percent	-10.29%	-7.86%

Method 2: We firstly use the optimization of OLHS method to generate 20 sample points, they are uniformly distributed in the design space; then we set Kriging approximation model to do the optimization calculation, this era is called 'era0'.In era 1,we add 4 new sample points according to the maximum 4 of WEIs(each Kriging model take 2)when different $\omega \in \{0.1, 0.2, 0.3, 0.4, 0.5, 0.6, 0.7, 0.8, 0.9\}$ are taken. Other eras can be done like 'era1'.We select the multi-objective genetic algorithm NSGA- II as the optimization method, and calculate the 300×200 individuals to get the optimization results. The Pareto fronts of each era can be seen in Figure 9. In Figure 9, 'era5' has 40 sample points and the 'norm' means the Pareto front of Method 1.

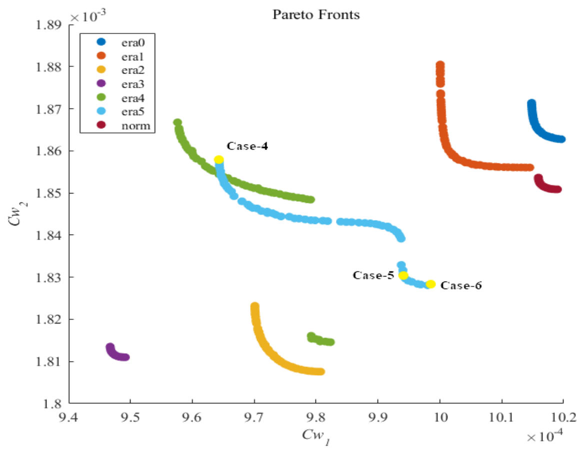

FIGURE.9 PARETO FRONTS OF METHOD 2

We can see that with the increase of the number of era, the Pareto front firstly has the trend of the lower-left movement, but then has the trend of upper-right movement, and the Pareto fronts of 'era4' and 'era5' seem to be very close. Note that the value coordinates with 0.001 as the unit. We can also see that although the Kriging model in Method 1 has high fidelity, it cannot find the real minimum cause the minimum value is obtained near the boundary, and the traditional Kriging model can't ensure high accuracy near the boundary. Fortunately, the EGO method considering WEI can help solve it cause it's feasible to add new sample points in order to find the minimum of the objective functions. Taking the computational cost into consideration, we suspend the calculation in 'era5', and choose 3 schemes from the Pareto front, and mark them as Case-4, Case-5 and Case-6 in the diagram.

We can finally see the cross validation of the eras in order to ensure their fidelity.

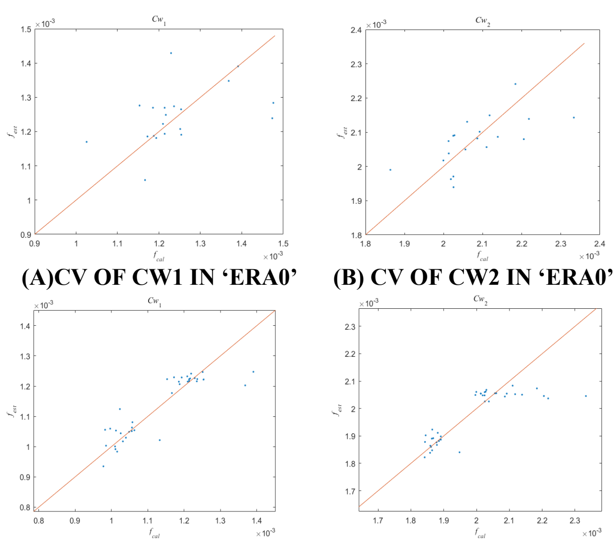

(A)CV OF CW1 IN 'ERA0' (B) CV OF CW2 IN 'ERA0'

(C) CV OF CW1 IN 'ERA5' (D) CV OF CW2 IN 'ERA5'

FIGURE.10 CV OF METHOD 2 IN DIFFERENT ERAS

TABLE.3 VARIANCES OF METHOD 2 IN DIFFERENT ERAS

era	sample points	variance	
		C_{w1}	C_{w2}
0	20	1.05E-08	6.00E-09
1	20+4	6.27E-09	3.79E-09
2	20+8	4.27E-09	2.88E-09
3	20+12	7.11E-09	5.81E-09
4	20+16	6.75E-09	5.44E-09
5	20+20	5.77E-09	5.09E-09

TABLE.4 OPTIMIZATION RESULTS CORRESPONDING TO THE INITIAL HULL IN METHOD 2

	C_w (Fr=0.26)	C_w (Fr=0.35)
Initial	0.001211	0.002076
Case-4	0.001028	0.001894
Decrease percent	-15.10%	-8.75%
Case-5	0.001009	0.001846
Decrease percent	-16.73%	-11.05%
Case-6	0.001012	0.001841
Decrease percent	-16.50%	-11.29%

Take Case-5 as an example for further analysis.

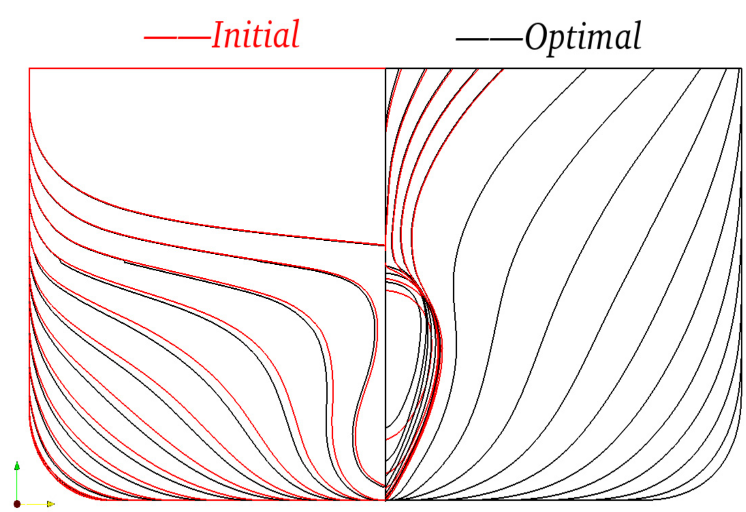

FIGURE.11 HULL LINE COMPARISONS OF CASE-5 IN METHOD 2

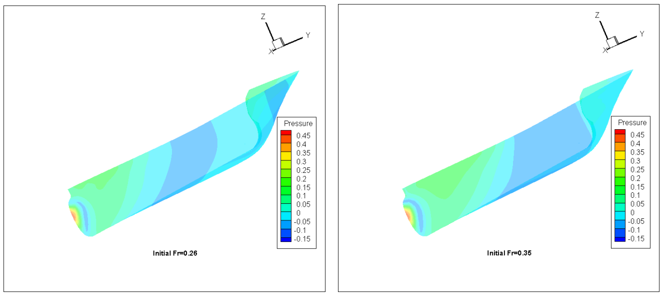

FIGURE.12 PRESSURE DISTRIBUTIONS OF INITIAL SHIP

From Figure 11, the bulbous of the optimal hull is thinner and higher than the initial one in order to decrease the ship wave, and stern parts of the optimal hull is a little fatter than the initial one. From Figure 12-13, the bulbous of the optimal hull has smaller high pressure and low pressure regions, which mean the lower wave-making resistance. From Figure 14, the free surface elevations of the optimal hull are smaller, especially in Fr=0.26, which also mean the lower wave-making resistances.

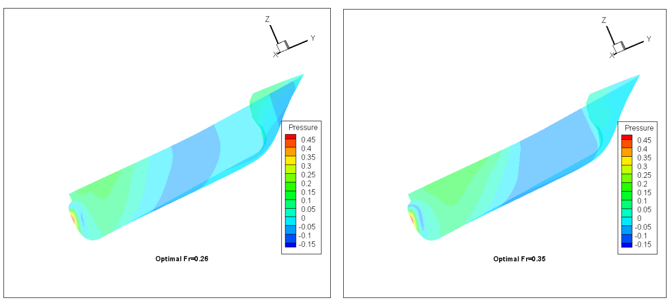

FIGURE.13 PRESSURE DISTRIBUTIONS OF OPTIMAL SHIP OF CASE-5

From Figure 11, the bulbous of the optimal hull is thinner and higher than the initial one in order to decrease the ship wave, and stern parts of the optimal hull is a little fatter than the initial one. From Figure 12-13, the bulbous of the optimal hull has smaller high pressure and low pressure regions, which mean the lower wave-making resistance.

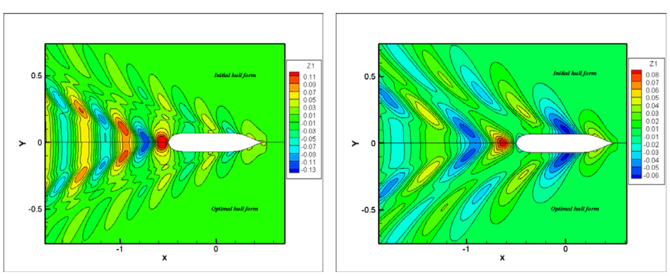

FIGURE.14 COMPARISONS OF FREE SURFACE ELEVATIONS OF INITIAL SHIP AND OPTIMAL SHIP OF CASE-5

From Figure 14, the free surface elevations of the optimal hull are smaller, especially in Fr=0.26, which also mean the lower wave-making resistances.

CONCLUSIONS

This paper presents a Kriging-based global optimization method efficient global optimization(EGO) considering WEI, which is different from the traditional optimization method. By this method, not only the accuracy of surrogate model is ensured but also we can find the real minimum objective functions. The method is successfully applied to the test functions and ship hull form optimization design. In future, it can be used to the ship hull form optimization via high-fidelity CFD methods, which will save much more cost, and can also improve the comprehensive hydrodynamic performance of ship hull form.

ACKNOWLEDGMENTS

This work is supported by the National Natural Science Foundation of China (51490675, 11432009, 51579145), Chang Jiang Scholars Program (T2014099), Shanghai Excellent Academic Leaders Program (17XD1402300), Program for Professor of Special Appointment (Eastern Scholar) at Shanghai Institutions of Higher Learning (2013022), Innovative Special Project of Numerical Tank of Ministry of Industry and Information Technology of China (2016-23/09) and Lloyd's Register Foundation for doctoral student, to which the authors are most grateful.

REFERENCES

[1] Jianwei Wu, Xiaoyi Liu, Min Zhao, Decheng Wan. Neumann-Michell theory-based Multi-objective Optimization of Hull Form for a Naval Surface Combatant[J]. Applied Ocean Research, 2017, 63: 129-141.

[2] Jones D R. Efficient Global Optimization of Expensive Black-Box Functions[J]. Journal of Global Optimization, 1998, 13(4): 455-492.

[3] Morris M D, Mitchell T J. Exploratory Designs for Computational Experiments [J]. Journal of Statistical Planning & Inference, 1992, 43(3):381-402.

[4] Kuhnt S, Steinberg D M. Design and Analysis of Computer Experiments[J]. Asta Advances in Statistical Analysis, 2010, 94(4): 307-309.

[5] Sykulski A M, Adams N M, Jennings N R. On-Line Adaptation of Exploration in the One-Armed Bandit with Covariates Problem[C]//Ninth International Conference on Machine Learning and Applications. IEEE, 2011: 459-464.

[6] Dixon L, Szego G P. The Optimization Problem: An Introduction[B]. 1978.

[7] Sederberg T W, Parry S R. Free-form Deformation of Solid Geometric Primitives[J]. Computers & Graphics, 1986, 20(4): 151-160.

[8] Sederberg T W, Parry S R. Comparison of Three Curve Intersection Algorithms [J]. Computer-Aided Design, 1986, 18(1): 58-63.

[9] Noblesse F, Huang FX, Yang C. The Neumann-Michell Theory of Ship Waves[J]. Journal of Engineering Mathematics, 2013, 79(1): 51-71.
[10] Chengliang Zhang, Jiayi He, Chao Ma, Decheng Wan. Validation of the Neumann-Michell Theory for Two Catamarans. [C]// Proceedings of the Twenty-fifth International Ocean and Polar Engineering Conference,2015.
[11] Xiaoyi Liu, Min Zhao, Decheng Wan, Jianwei Wu. Hull Form Multi-Objective Optimization for a Container Ship with Neumann Michell Theory and Approximation Model [J]. International Journal of Offshore and Polar Engineering， Vol.27, No.4, 2017, pp. 423-432
[12] Chi Y, Huang F, Noblesse F. Practical evaluation of the drag of a ship for design and optimization[J]. Journal of Hydrodynamics, 2013, 25(5): 645-654.
[13] H. Kim, C. Yang, H.H. Chun. Hydrodynamic optimization of a modern container ship using variable fidelity models. [C]//19th International Offshore and Polar Engineering Conference, Osaka, Japan, 2009.
[14] Xinwang Liu, Decheng Wan. Numerical Analysis of Wave Interference Among the Demihulls of the High-Speed Quadramarans[J]. Shipbuilding of China, 2017, Vol.58, Special 1, pp.140-151

